

INVESTIGATION ON REACTIVE SINTERING  
OF NIOBIUM TRIALUMINIDE, NbAl<sub>3</sub>Paulo Iris Ferreira  
Ricardo M. Leal NetoComissão Nacional de Energia Nuclear  
Instituto de Pesquisas Energéticas e Nucleares  
P.O.Box 11049 - São Paulo - Brazil  
Telefax 212-3546 Telephone (011) (211-6011)

## ABSTRACT

The intermetallic NbAl<sub>3</sub>, one of the compounds present in the Nb-Al system, has recently gained increased attention since its physical properties are very convenient when structural applications at high temperature are envisaged. Though various routes have been utilized for the synthesis of this compound, the reaction sintering of the elemental powders appears to be a very practical way for this purpose and is focussed in this work. The influences of the elemental powders particle size distribution, compact composition and the reaction sintered thermal cycle on the sintered pellet porosity, microhardness and microstructure were investigated. The experimental results are present and discussed. A tentative model to explain reaction sintering of niobium aluminides is proposed.

## 1. INTRODUCTION

Ordered intermetallic aluminides are regarded as potential materials for structural applications at high temperature due to their excellent corrosion resistance, relatively low density and high mechanical strength in a wide range of temperatures (1,2). However, the low ductility, the tendency to brittle fracture and the environmental sensitivity of the mechanical strength, generally observed in these alloys, have restricted its practical use (1,2,3,4).

Several investigations carried out in the last decade have shown that many of these limitations could be attenuated, or even eliminated, through macroalloying and microalloying processes and thermal-mechanical treatments (1,2,5,6). These findings have renewed interest on the physical metallurgy of these alloys and, as a consequence, a impressive number of research work in this area is now being done worldwide.

Various routes have been undertaken for the fabrication of intermetallic alloys including conventional melt-casting-working (7,8,9), rapid solidification (10,11,12) and powder metallurgy process (13,14,15). In this universe of processes, conventional powder metallurgy is an important mean for the obtainment of high performance complex geometry components. In general, rapidly solidified prealloyed intermetallic powders or ribbons are used as starting materials and consolidation is accomplished by hot extrusion or hot isostatic pressing. Although this approach is well established, it involves long process cycles and high sintering temperatures at considerably high costs.

An alternative powder processing technique known as reaction sintering, combustion synthesis or self-propagating high temperature synthesis is gaining increased attention (16,17,18,19). An extensive review on this subject was reported by Munir and Anselmi - Tamburini (20). By this methods compounds with a sufficiently negative formation enthalpy can be synthesized through an exothermic reaction between its elemental powders. Low processing temperatures, short processing times, relatively inexpensive equipment and a great flexibility for composition and microstructure control, make this alternative very attractive. Recent investigations have demonstrated the success of the reaction sintering for fabricating near full density nickel, iron and niobium aluminides (21,22,23). The Nb-Al phase diagram is characterized by the presence of three intermetallic phases  $Nb_3Al$ ,  $Nb_2Al$  and  $NbAl_3$ . The  $NbAl_3$  compounds presents a low density ( $4.54g/cm^3$ ) and a high melting point ( $1680C$ ) (24,25). Attention has been focussed on  $NbAl_3$  mainly due to its use as a protective coat in Nb and its alloys, since the brittleness, associated with its  $DO_{22}$  structure, has restricted its use in structural components. Recently, renewed attention has been directed towards Niobium aluminides with emphasis on mechanical properties improvement. The objective of the present research was to investigate the use of exothermic reactions to elaborate niobium aluminides from elemental powders. Fine Nb and Al powders were used to promote compound formation. The effects of processing variables on the reaction sintering process were studied for the  $NbAl_3$  composition. The influence of compact stoichiometry on the characteristics of reaction sintered pellets was investigated for aluminum content in the range 42 at% - 75 at%. Microestructural characterization and limited mechanical property measurements were carried out on reaction sintered pellets.

## 2. EXPERIMENTAL

Figure 1 shows a schematic representation of the procedure used in this work for the reaction sintering of niobium aluminides. Commercial gas atomized aluminum (ALCOA) and hydride-dehydride niobium (FTI-Lorena) powders were initially size classified by sieving and divided into the fractions of interest. The particle size distribution for each fraction selected was determined using a sedigraph and is shown in figure 2. Scanning Electron Microscopy was utilized for the characterization of the powder morphology. Figure 3 show electron micrographs illustrating typical morphology of the niobium and aluminum powders. Aluminum particles present a round and ligamental shape with a number of small satellites on the surface. Niobium particles have an angular shape characteristic of the hydride/dehydride process.

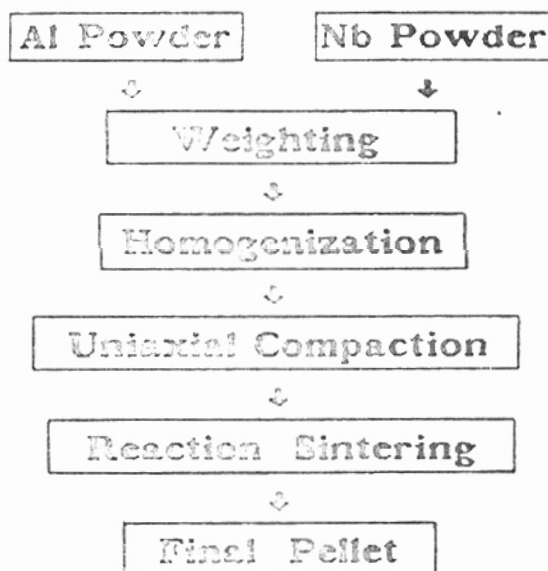


Figure 1- Schematic diagram illustrating the procedure used for the reaction sintering experiments.

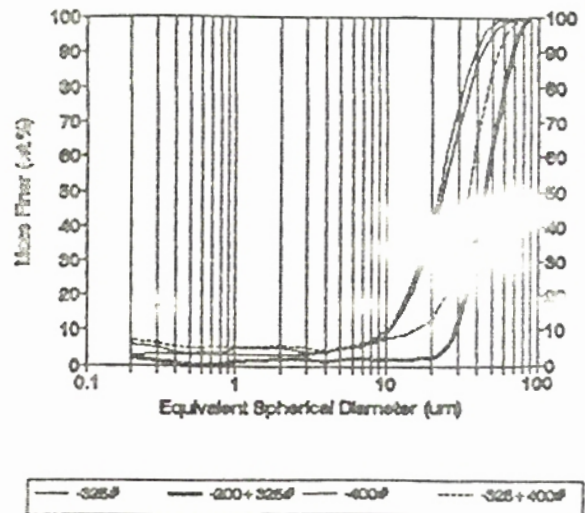
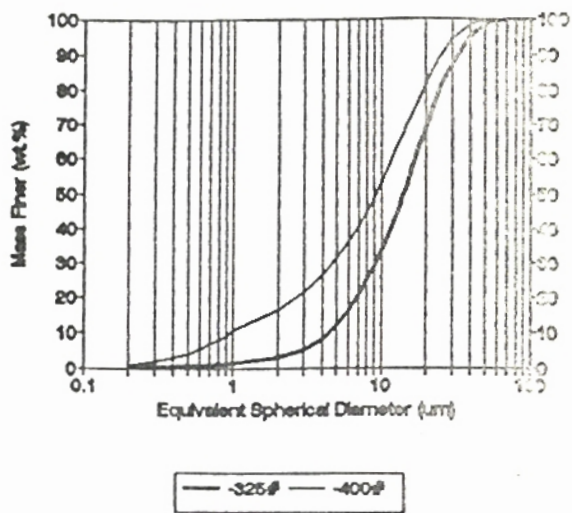
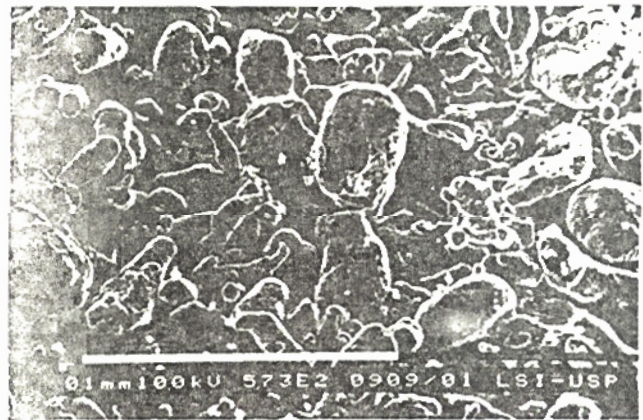


Figure 2- Particle size distributions obtained for the various powder fractions utilized: (a) Niobium powder; (b) Aluminum powder.



(a)



(b)

Figure 3- SEM micrographs of the as received powder: (a) niobium; (b) aluminum.

After classifying and analysing, the powders were weighted in the desired proportion  $m_{Al}/m_{Nb} = X$  ( $m_{Al}$  and  $m_{Nb}$  are the weights of aluminium and niobium, respectively) and mixed. The value of  $X$  was varied from  $X=0.21$  to  $X=0.87$ , which corresponds to aluminide composition ranging from 17.38 wt.% Al (42 at.% Al) to 46.55 wt.% (75 at.% Al), respectively.

The Al and Nb powder mixtures were individually homogenized in air using an equipment Turbula operating at 35 rpm for 10 minutes. These conditions were seen to be appropriate for the homogenization of the mixture of the various powder size distributions utilized. After this procedure, the powder mixtures were compacted at room temperature in an uniaxial press using a double action die and applied pressure ranging from 200 to 400 MPa. A solution containing stearic acid and acetone was used for die lubrication. Green compacts with 14 mm external diameter and height around 6 mm were obtained.

Reaction sintering of the compacts was realized in a tubular furnace containing a moveable quartz chamber. The green compact was initially positioned in the interior of the chamber and the whole system was evacuated until pressures of  $10^{-5}$  Torr were reached. The chamber containing the compact was then introduced in the furnace before heating to the temperature  $T$ . Compact and furnace temperatures were continuously monitored and controlled with thermocouples. In all experiments a heating rate of 15C/min was utilized. During the exothermic reaction, a certain amount of heat is liberated leading to an increase in the compact temperature and a rapid transient in the vacuum level. The reacted compacts were kept in the furnace at the set temperature for 60 minutes, and then cooled under vacuum by taking the quartz chamber off the furnace.

Longitudinal sections of the reaction sintered pellets were used for metallographic observations. The polished surfaces were analysed using normal and polarized light techniques to reveal porous and grain structures, respectively.

Scanning Electron Microscopy, X-ray diffraction and Electron microprobe analysis were used for the characterization of the phases present in the sintered pellets as well as their distribution. The bulk density of the pellets was determined by immersion technique. Total porosity could then be determined. Closed porosity was measured by helium pycnometry.

### 3. EXPERIMENTAL RESULTS

#### -Reaction Sintering Aspects for $NbAl_3$ composition.

The reaction sintering process was initially analysed by differential thermal analysis (DTA). A  $NbAl_3$  stoichiometric mixture of aluminum and niobium powder weighting 45.7mg was fed to the alumina crucible of a DTA equipment and slightly tapped. DTA experiment was run under argon atmosphere, to minimize oxidation effects, from 250C to 1200C at a heating rate of 15C/min. A similar heating program was conducted with empty crucibles to establish a reference.

The DTA curve obtained is presented in figure 4. The first endothermic peak refers to aluminum melting. The exothermic reaction starts at approximately 900C. Two peaks are clearly delineated: the first with maxima around 950C followed by the major peak around 1050C. X-ray diffraction analysis confirmed  $NbAl_3$  formation at the end of the exothermic reaction. This DTA curve was used as a reference for the planning of succeeding experiments.

Table I summarizes the experimental conditions used for the initial investigation of the effects of the processing variables on the reaction sintering characteristics of  $NbAl_3$  compound. The variables, Al and Nb powder particle size distribution, furnace set temperature, compacting pressure and the use of previous compact degassing before reaction, were focused.

Figure 5 shows typical macrographs of longitudinal sections of the reaction sintered pellets to illustrate the effects of processing variables on reaction sintering densification.

In general, compacting pressure had no noticeable influence on the final pellet characteristics, at least in the range of pressures utilized in table I.

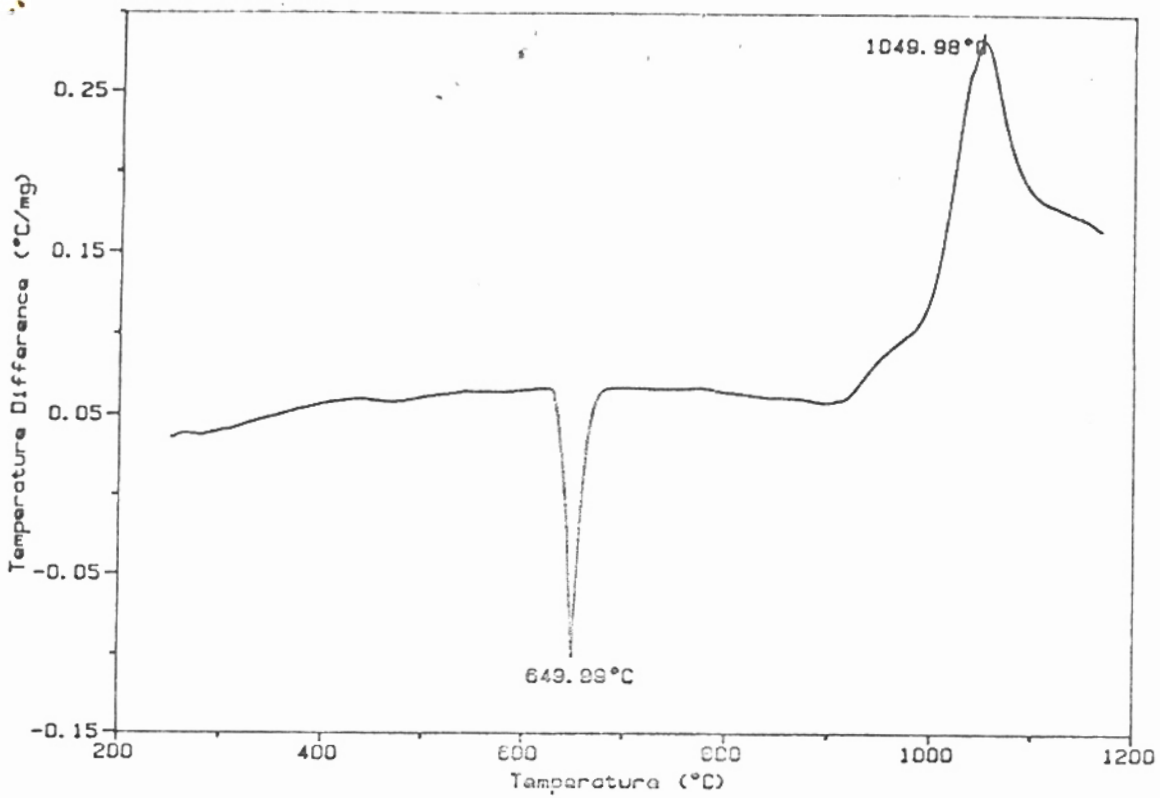


Figure 4- Differential Thermal Analysis (DTA) result obtained for Nb-Al mixture (75 at.% Al).

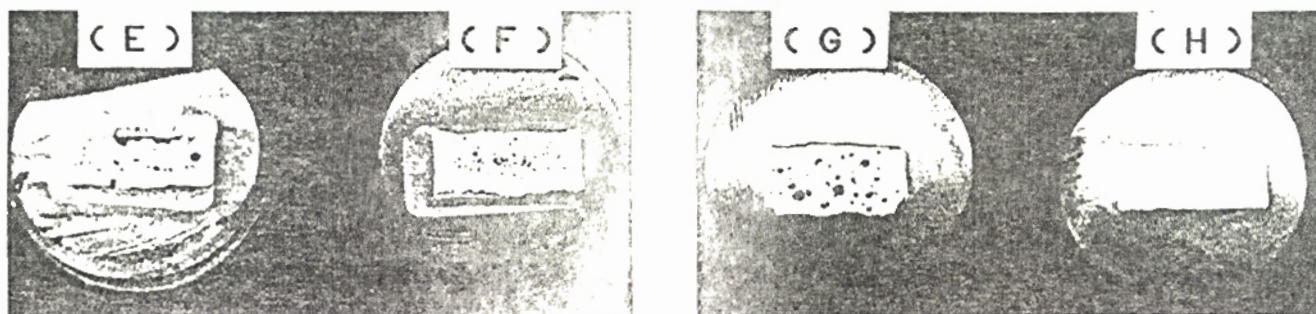
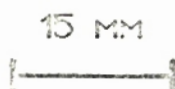
TABLE I - EXPERIMENTAL CONDITIONS USED TO INVESTIGATE THE EFFECTS OF PROCESSING VARIABLES ON NbAl REACTION SINTERING

PELLET GROUP	POWDER SIZE		TEMPERATURE TIME	COMPACTING PRESSURE (MPa)	DEGASSING (500°C/4h)	RELATIVE DENSITY
	Al	Nb				
A	-325# (24 μm)	-325# (15 μm)	900 °C/1H	200	NO	85%
				300	NO	92%
				400	NO	94%
B	-325# (24 μm)	-200# +325# (55 μm)	900 °C/1H	200	NO	88%
				300	NO	94%
				400	NO	96%
C	-325# (24 μm)	-325# (15 μm)	900 °C/1H	300	YES	92%
D	-400# (23 μm)	-400# (9 μm)	900 °C/1H	300	YES	92%
E	-200#+325# (45 μm)	-400# (9 μm)	1100 °C/1H	300	YES	92%
F	-325#+400# (35 μm)	-400# (9 μm)	1100 °C/1H	300	YES	92%
G	-325# (24 μm)	-325# (15 μm)	1100 °C/1H	300	YES	92%
H	-400# (23 μm)	-400# (9 μm)	1100 °C/1H	300	YES	92%



900°C - 1 H

NON DEGASSING		DEGASSING ( 500°C - 4 H )	
AL : 24 UM	AL : 24 UM	AL : 24 UM	AL : 23 UM
NB : 15 UM	NB : 55 UM	NB : 15 UM	NB : 9 UM



1000°C - 1 H

DEGASSING ( 500°C - 4 H )		DEGASSING ( 500°C - 4 H )	
AL : 45 UM	AL : 35 UM	AL : 24 UM	AL : 23 UM
NB : 9 UM	NB : 9 UM	NB : 15 UM	NB : 9 UM

Figure 5- Optical Macrographs of longitudinal sections of reaction sintered pellets processed for 1 hour at 900°C (A to D) and 1000°C (E to H). Compact degassing condition and average particle size of Al and Nb are indicated.

The influence of prior compact degassing on densification can be perceived through the observation of compacts fabricated under equal experimental conditions with average particles sizes of 24  $\mu\text{m}$  for Al and 15  $\mu\text{m}$  for Nb, reaction sintered at 900 C. The macrographs (A and C) clearly show that without a degassing step, large voids are formed and a general swelling of the reacted pellet takes place. Degassing leads to a considerable reduction in porosity and only a mild and uniform pellet swelling. Degassings at 500C for longer times were also utilized without any significant improvement on the final results.

The influence of aluminum and niobium particle sizes on the reaction development was investigated using groups E to H compacts (TABLE I). The green density was maintained at 92% of theoretical. All compacts were initially degassed at 500C/4h and then heated to 1100C under  $10^{-5}$  Torr vacuum under a heating rate of 15C/min. After the reaction transient the pellets were kept at 1100C/1 hour and cooled to room temperature. Figure 5 illustrate the final porosity of those sintered pellets. Pellets E, F and H for which niobium particle size was kept constant (9  $\mu\text{m}$ ) show that large aluminum particle size resulted in the formation of large voids. Those large voids are also present if niobium particle size is increased from 9  $\mu\text{m}$  to 15  $\mu\text{m}$ , as can be deduced from the comparison of results obtained for group G and H compacts. A similar behaviour is observed for non-degassed compacts of groups A and B reaction sintered at 900C. In the particular case of pellet B the reaction was not completed and unreacted niobium was left at the end, as confirmed by X-ray diffraction and microprobe analysis.

Furnace temperature when above 900C have only a small influence on the densification, contrary to that observed in classical sintering behavior. Once the exothermic reaction is initiated, the heat generated is sufficient for its self-propagation and for the increase in temperature to levels where densification occurs. An increased densification is observed when pellets are held at 1100C instead of 900C as illustrated in fig.5 for the compacts of group G,H and C,D, respectively.

#### - Effect of composition

The effects of stoichiometry on densification were investigated using compacts prepared with 23  $\mu\text{m}$  Al and 9  $\mu\text{m}$  Nb powder with a green density around 90% of theoretical. These compacts were also degassed at 500C/4 hours, heated in vacuum at 15K/min to 1100C and held for 1 hour. Figure 6 shows the total and closed porosities after reaction as a function of Al content.

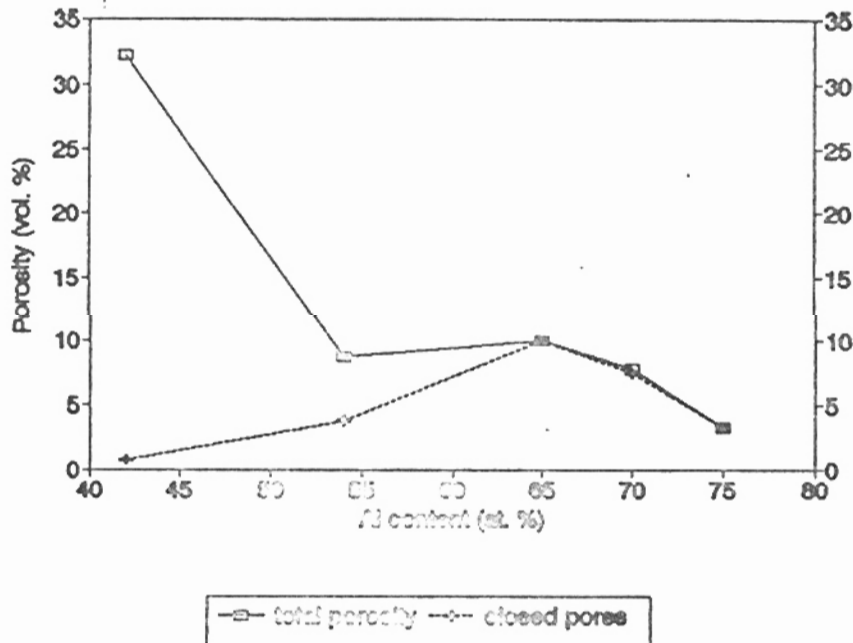


Figure 6- Total and closed porosity of reaction sintered pellets as a function of Al content in the Nb-Al compact.

Total porosity decreases continually from a value around 30% to values close to 4% when the aluminum content is varied from 42% to the stoichiometric  $\text{NbAl}_3$  composition. Helium pycnometry data indicate that for compositions above the eutectic (54 at% Al), the majority of pores are closed in nature, whereas for lower aluminum content interconnected porosity predominates.

Typical microstructures, observed under normal and polarized light conditions, for the pellets containing 42 at.%, 54 at.%, 65 at.% and 75 at.% Al are presented in figure 7. The pore structure occurring in the 75 at.% Al pellet (figure 7) is characterized by a bimodal distribution: large pores with an average size around 50  $\mu\text{m}$  and very fine pores nearly 2  $\mu\text{m}$  in size located preferentially at grain boundaries. When the aluminium content of the compact is decreased from 75 at.% ( $\text{NbAl}_3$  stoichiometry) towards  $\text{Nb}_2\text{Al}$  composition, there is a tendency to increase the amount and size of fine pores which results in a sponge-like structure at 42 at.%.

The major phase occurring at 75 at.% Al is the  $\text{NbAl}_3$  phase, as verified by X-ray diffraction and microprobe analysis. However,  $\text{Nb}_2\text{Al}$  phase is also observed in small areas, with an eutectic like structure, mainly located at triple grain boundary joints, as indicated by arrows in figure 7a and figure 8a. Two phases,  $\text{NbAl}_3$  and  $\text{Nb}_2\text{Al}$ , are always present in the microstructure of pellets with lower aluminum content.

Decreasing the amount of aluminum in the compact result in reduction on  $\text{NbAl}_3$  and increase on  $\text{Nb}_2\text{Al}$  volume fractions. Volume fractions determined for each composition are consistent with values calculated from equilibrium phase diagram. This aspect can be visualized in figure 7 (a to d). The  $\text{Nb}_2\text{Al}$  phase is distributed in the microstructure in a thin slab along  $\text{NbAl}_3$  grain boundaries (figure 8b) at 70 at.% Al. Furthermore, the  $\text{NbAl}_3$  grains become increasingly spherical in shape. At 65 at.% Al the microstructure can be viewed as constituted of roundy  $\text{NbAl}_3$  particles dispersed in a continuous  $\text{Nb}_2\text{Al}$  matrix as illustrated in figures 7c and 8c. Compacts with composition below eutectic (54 at.% Al) result in sintered pellets with microstructure containing large continuous areas of  $\text{Nb}_2\text{Al}$  phase surrounded by  $\text{NbAl}_3$  grains in a neck-lace disposition as seen in figures 7d and 8d. It is interesting to note that there is a clear reduction of  $\text{NbAl}_3$  grain size in the sintered pellet when the amount of Al is decreased from 75 at.% to 42 at.% as illustrated in figure 9.

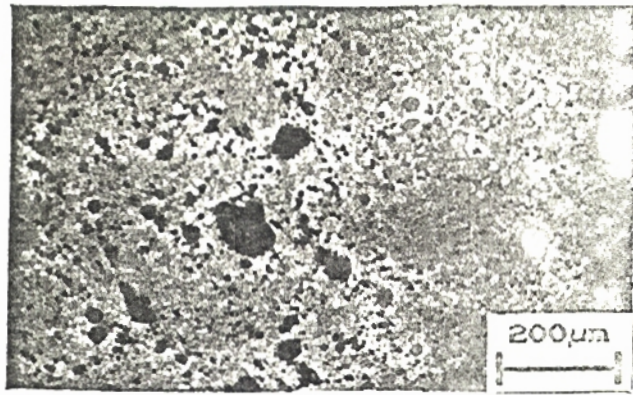
#### - Microhardness Measurements

Microhardness measurements were performed on reaction sintered pellets using a Vickers diamond pyramidal indenter with a 100g load. Higher loads were seen to induce cracks around indentation and unacceptable fluctuation of the results. Hardness values were affected by pellet porosity. However, reliable data (taken at low porosity areas of the sample) were obtained for pellets reaction sintered at 1100C. These values were ( $544 \pm 92$ ), ( $593 \pm 65$ ), and ( $650 \pm 64$ ) for  $\text{NbAl}_3$  pellets of the conditions E, F and H, respectively. Although the data show some dispersion, a perceptible decrease of hardness with increasing porosity can be verified. The value measured for the 96% dense pellet, H, exceeds the value 509 (measured with 200g load) reported by Murray and German (23) for reactive hot isostatic pressed 98% dense  $\text{NbAl}_3$  pellets. The reasons for this discrepancy are not clear at this point.

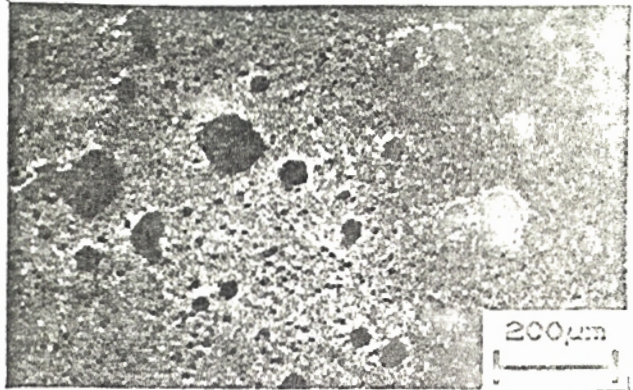
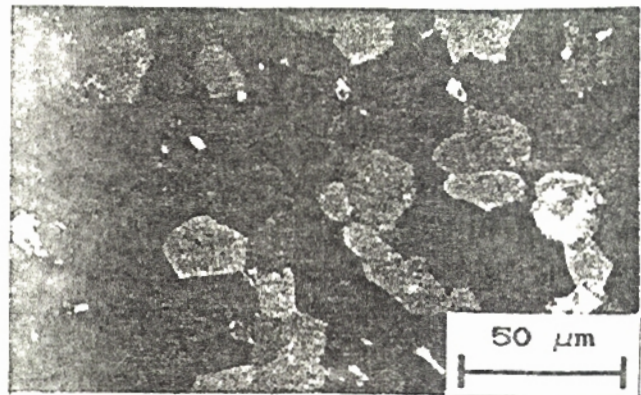
The variation of microhardness with aluminum content is shown in figure 10. The low value at 42 at.% Al reflects the high porosity of the specimen, as shown in figure 6. For the other points in figure 10 porosity is relatively low and its effect on hardness can, in principle, be neglected. Therefore, when the pellet aluminum content is decreased the hardness increases towards values around 800. This increase in hardness is associated with an increased volume fraction of  $\text{Nb}_2\text{Al}$  phase and a reduced  $\text{NbAl}_3$  grain size in the pellet, as can be seen in figure 8 and figure 9.

Normal Light

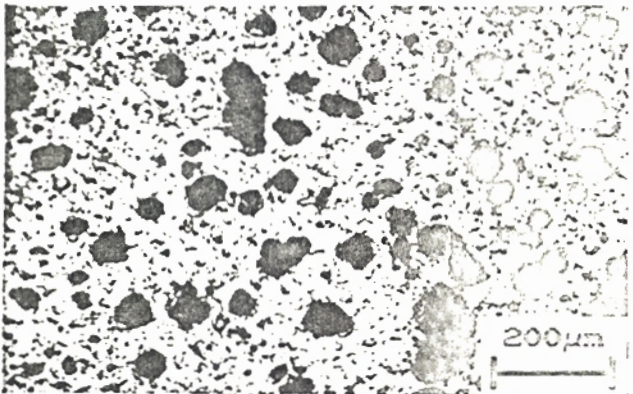
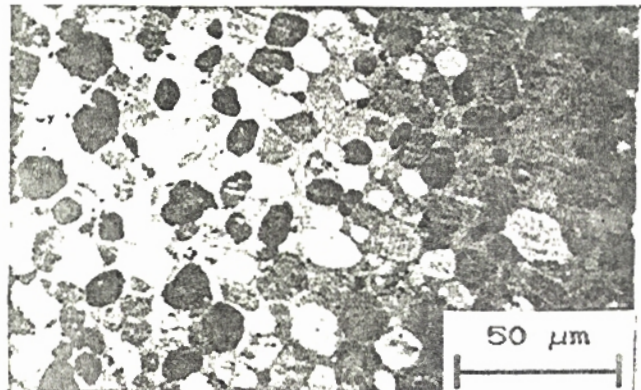
Polarized Light



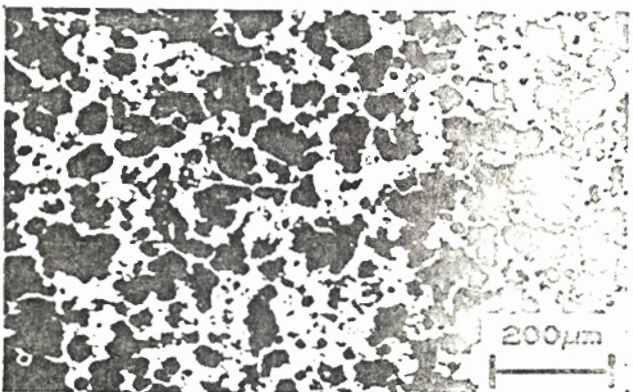
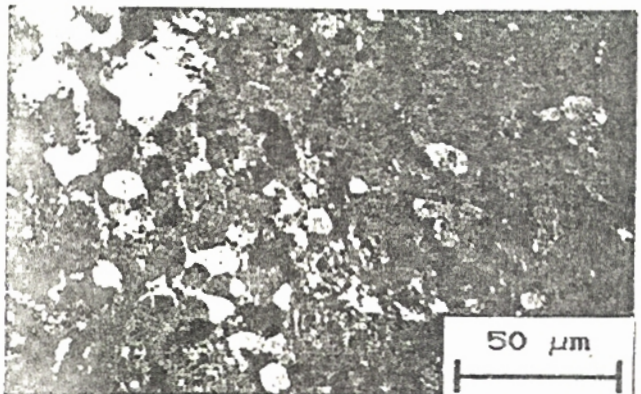
(a)



(b)



(c)



(d)

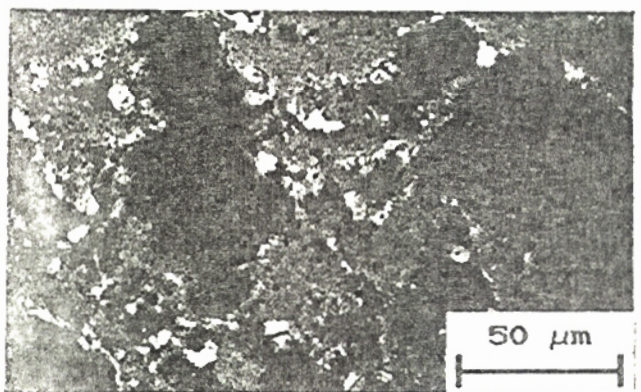
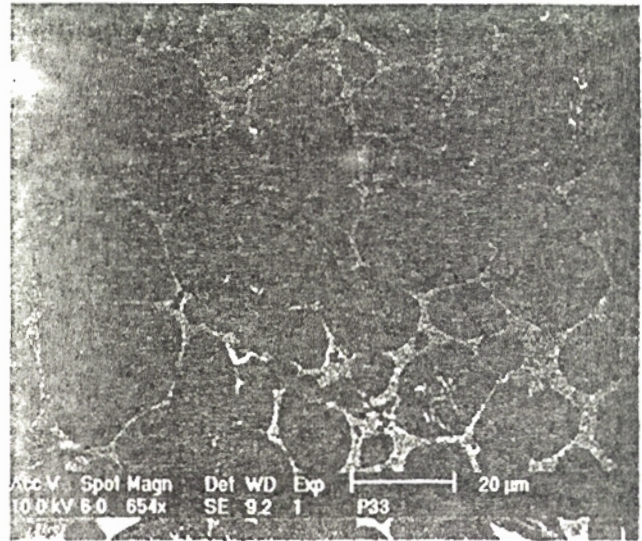


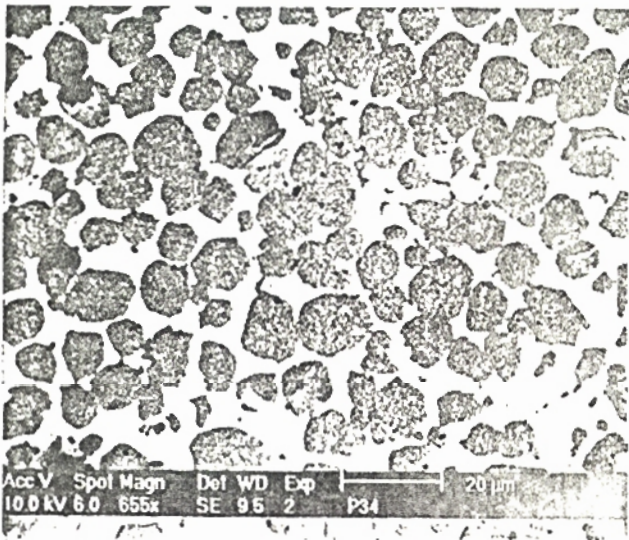
Figure 7- Optical micrographs taken under normal and polarized light, illustrating typical microstructures of sintered pellets with compositions: (a) 75% at.% Al; (b) 65 at.% Al; (c) 54 at.% Al; (d) 42 at.% Al.



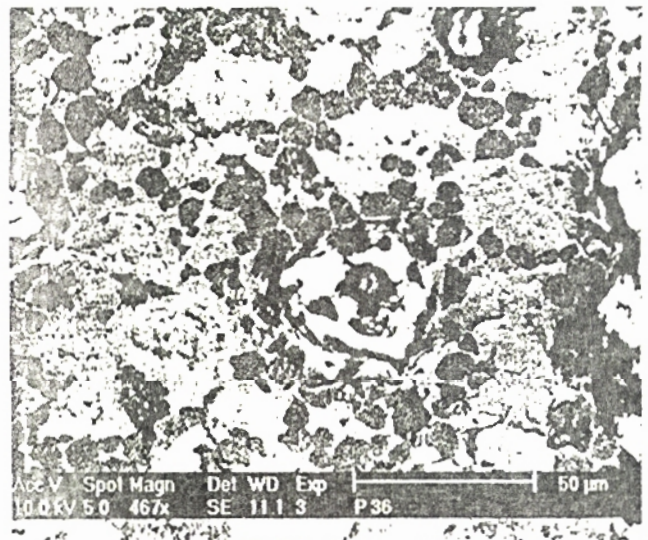
(a)



(b)



(c)



(d)

Figure 8- SEM micrographs showing microstructural aspects of reaction sintered pellets: (a) 75 at.% Al; (b) 70 at.% Al; (c) 65 at.% Al; (d) 54 at.% Al. (Dark areas:  $\text{NbAl}_3$ ; Light areas:  $\text{Nb}_2\text{Al}$ ).

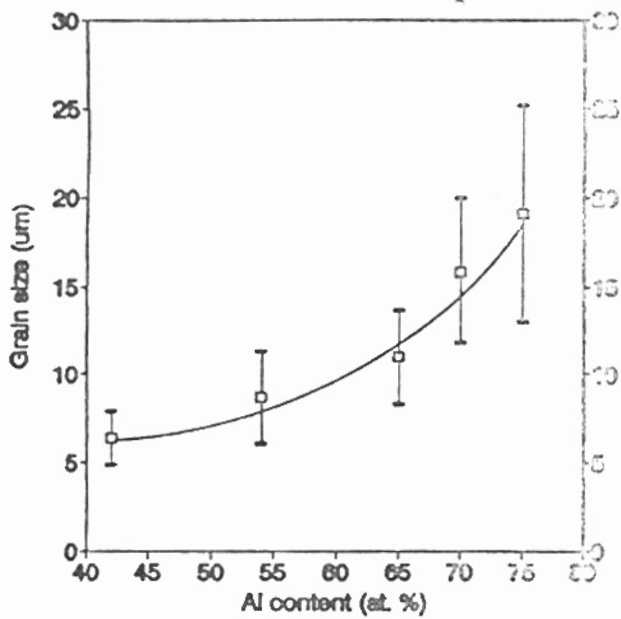


Figure 9- Average grain size of  $NbAl_3$  phase present in reaction sintered pellets as a function of Al content of the Nb-Al compact.

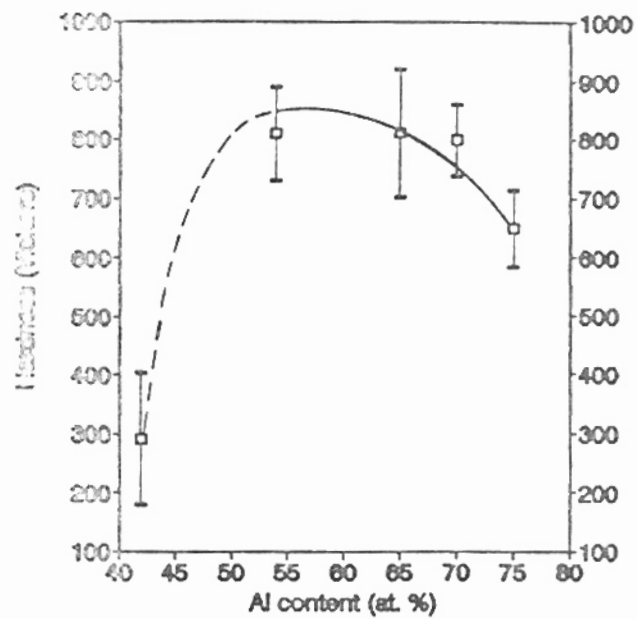


Figure 10- Vickers microhardness of reaction sintered pellets as a function of Al content in the Nb-Al compact.

#### 4. DISCUSSION

Transient liquid phase sintering mechanisms have been recalled to help explain the reaction sintering process (21,22,23). An important requirement for the densification is the presence of a wetting liquid during the reaction. The amount, duration and distribution of the liquid phase at the reaction zone will determine the final sintered density. In reaction sintering the liquid phase has an extremely short existence, confined to the passage of the reaction front. The quantity of liquid available at the reaction zone depends essentially on compact composition. The distribution of the liquid phase in the microstructure is strongly dependent on the Nb:Al particle size ratio, since this ratio affects the interconnectivity of the niobium and aluminum phases. Interconnectivity of the two phases helps capillary action of the molten aluminum phase. It is believed that capillarity forces the structure together at the initial stages of the reaction resulting in higher final sintered density.

The results presented in figure 5 were obtained using the following Nb:Al particle size ratios: 1:1.6 (compact A); 1:0.4 (compact B); 1:1.5 (compacts C and G); 1:2.6 (compacts D and H); 1:5 (compact E); and 1:3.9 (compact F). According to a model proposed by Kusy (26), interconnectivity of the aluminum and niobium phases for  $NbAl_3$  stoichiometry (73 vol.% Al in the compact) occurs when Nb:Al = 1:3. In this work optimum densification took place in situations D and H for degassed compacts processed at 900 C and 1100C, respectively, where Nb:Al = 1:2.6. Similar results were reported by Murray and German (23) for a Nb:Al ratio of approximately 1:3. These results indicate that the interconnectivity of phases may play one important role on the mechanism of reaction sintering densification. However, the absolute values of the particle size of each phase also affect densification, since diffusion times involved in the reaction may not be sufficient for reaction completeness when large particles are used.

An attempt to explain the present observations on reaction sintering Nb-Al compacts can be advanced. During the initial heating of the Nb-Al compact, aluminum rich zones are preferentially formed in the Nb particles starting at the point of contact between Al and Nb particles. Low solid state solubility of niobium in aluminum as indicated by the equilibrium phase diagram (25), as well as, the fact that the diffusion coefficient of aluminum in niobium and/or niobium compounds is greater than that of Nb in Al (27) would justify this unbalanced atom flux. Solid state nucleation and growth of compounds can, therefore, occur at aluminum-niobium interparticle contacts during heating. Experiments performed by Slama and Vignes (27) showed that  $NbAl_3$  compound is first nucleated at these contact points. These points will certainly be favored sites for initial aluminum melting since localized additional heating occurs when compound is being formed. Liquid aluminum pools formed at these sites are quickly sipped to empty spaces nearby by capillary action. Liquid aluminum covers the available surface of the niobium particles. At this stage  $NbAl_3$  nuclei exists in the compact in equilibrium with local molten aluminum and unreacted solid aluminum and niobium.

When the temperature of compact is increased, the solubility of niobium in liquid aluminum increases. Niobium dissolution in liquid aluminum occurs. Growth of  $NbAl_3$  nuclei would happen simultaneously either by consumption of the niobium enriched liquid or by eventual aluminum diffusion to the interface Nb- $NbAl_3$ . The first exothermic peak observed in DTA curve (figure 4) at around 950C could be associated to these events. Once a small quantity of Nb enriched liquid is formed, a rapid increase in the reaction rate takes place. As the temperature of the compact is raised, more enriched liquid is formed with supplementary increase in reaction rate, in such a way as to end in reaction self propagation (main peak in DTA curve).

The very high speed of the overall process suggests that initial  $NbAl_3$  nuclei existing at Nb-Al interparticle contacts, grow mainly by using the niobium enriched liquid until all reagents are consumed. Occasionally, local unbalanced supersaturated niobium enriched liquid can be trapped at interstices between impinging  $NbAl_3$  particles. These liquid pools could be responsible for the eutectic like structure ( $Nb_2Al-NbAl_3$ ) observed at  $NbAl_3$  triple grain boundary joints (figure 8a).

According to this model outward currents of liquid aluminum would be flowing from the original aluminum particle sites. Also, a niobium enriched aluminum current would be flowing in the opposite direction on the  $NbAl_3$  particles surface. Neighbouring  $NbAl_3$  particles grow and contact. As a consequence, gross pores will be left at original aluminum particle sites. Furthermore, fine porosity can occur at  $NbAl_3$  grain boundaries due to the presence of entrapped liquid when  $NbAl_3$  particles touch each other.

The present results are consistent with the proposed explanation. In fact, on increasing the aluminum particle size at fixed niobium particle size (compacts H,F and E) the average size of the large pores observed in the microstructure also increase as expected. Another important point is that the fine porosity is almost exclusively located at  $NbAl_3$  boundaries (figures 7a, and figure 8b,c). This reinforces the idea that  $NbAl_3$  grains grow using the niobium enriched liquid.

When the amount of niobium in the compact is increased, at least two things are expected. First, the niobium content of the liquid phase would increase to values required for  $Nb_2Al$  formation. Growth of this phase should occur intergranularly. In fact  $Nb_2Al$  occurs intergranularly as illustrated in figure 8b and 8c. Secondly, the number of Al-Nb interparticle contacts increases. Therefore, a larger number of  $NbAl_3$  nuclei shall be present in the compact during the initial stage of reaction sintering. These nuclei will be competing for less available aluminum to grow, resulting in reduced final  $NbAl_3$  grain size. This would explain the decrease on the final  $NbAl_3$  grain size shown in figure 9 when the amount of niobium in the compact is increased.

## 5. CONCLUSIONS

Reaction sintering was investigated as a pressureless process to synthesize high density niobium aluminides based upon  $NbAl_3$  stoichiometry. Compound synthesis occurs within seconds during rapid compact heating associated with the exothermic reaction. Best results were obtained with the following experimental conditions: a Nb:Al particle size ratio equal to 1:2.6; a heating rate of 15C/min; a holding time at temperature of 1100C/1 hour; a degassing step at 500C/4h; and a vacuum level of  $10^{-5}$  Torr. Microstructure of these 96% dense pellets is essentially characterized by the presence of  $NbAl_3$  grains; a very small quantity of  $Nb_2Al$  phase is also observed at triple grain

boundaries. The effect of compact composition was investigated for aluminum content varying from 42 at.% to 75 at.%. Two phases,  $NbAl_3$  and  $Nb_2Al$ , are simultaneously synthesized when the niobium content of the compacts is increased towards the  $Nb_2Al$  stoichiometry.  $NbAl_3$  phase is seen to nucleate first at niobium-aluminum interparticle contacts.  $Nb_2Al$  phase occurs in between the  $NbAl_3$  grains when compact compositions are above the eutectic. Below the eutectic composition,  $NbAl_3$  grains were seen to be pushed to  $Nb_2Al$  grain boundaries during solidification forming a neck-lace distribution. Reaction processed pellets showed measured microhardness values significantly higher than a previous reported value.

## 6. BIBLIOGRAPHY

1. High Temperature Ordered Intermetallic Alloys, Proc. Materials Research Society Symposium, Boston, vol.39, C.C.Koch, C.T.Lia, and N.S. Stoloff, Ed. MRS Pub., Pittsburgh, (1985).
2. High Temperature Ordered Intermetallic Alloys II, Proc. Materials Research Society Symposium, Boston, vol.81, N.S.Stoloff, C.C.Koch, C.T.Liu and O.Izumi, Ed., MRS Publication, Pittsburgh, (1987).
3. N.S. Stoloff and R.G. Davies, Progr. Mat. Sci, vol.13 (1), (1966), 1.
4. M.J. Marcincowsky in Treatise on Mat.Sci. and Technology, H.Herman, Ed., Academic Press, vol.5, (1974), 181.
5. C.T.Liu, "Ordered Intermetallic Alloys - Brittle Fracture and Ductility Improvement", in Science of Advanced Materials, H.Weidenschich and M.Meshii, Ed., ASM International Publication, USA, (1990), 423.
6. M.H.Yoo - "Deformation and Fracture of Ordered Intermetallic Compounds, ibid, p.461.
7. C.T.Liu, C.L.White, Acta Metall., vol.35, (1987), 643.
8. T.Kakassugi, O.Izumi, and N. Masahashi, Acta Metall. vol.23, (1985), 1259.
9. G. Sauthoff, Zeitschrift fur Metallkunde, vol.81, nr.12, (1990), 855.
10. C.C. Koch, Int. Metall. Reviews, vol.33, nr.4, (1988), 201.
11. S. Noursbakhsh and P.Chen, Acta Metall., vol.37, (1989), 1373.
12. P.I.Ferreira and G.M. Gonçalves, Proc. Annual Congress of the Brazilian Society for Metals (ABM), Brazil, vol.4 (1990), 469.
13. E.M. Schulson, The Int.J. of Powder Metall., vol.23, n.r.1, (1987), 25.
14. K. Vedula and J.R. Stephens; Powder Metallurgy 1986- State of the Art, W.J. Huppman, W.A. Kaysser and G.Petsow, Ed., Verlag Schmid, Freiburg, west German, (1986), 205.
15. I.Baker, F.S. Ichishita, V.A. Surpreant and E.M. Schulson, Metallography, vol.17, (1984), 299.
16. A.Bose, B.W.Rabin and R.M. German, Powder Metall. Intern., vol.20, (1988), 25.
17. D.M. Bowden, P.J. Meschter, L.H.Yu, M.A.Meyers, N.M.Thadhani, Journal of Metals, vol.40, (9), (1988), 18.
18. R.M.Leal Neto and P.I.Ferreira, Proc. Powder Metall.Seminar, Brazilian Society for Metals (ABM), S.Paulo, Brazil, (1991), 399.
19. Z.A.Munir, Ceramic Bulletin, vol.67, (2), (1988), 342.
20. Z.A.Munir and V.Anselmi - Tamburini, Materials Science Reports, vol.3, (7), (1989), 277.
21. D.M.Sims, A.Base and R.M. German, Progress in Powder Metallurgy, vol.43, 9, (1987), 575.
22. B.H.Rabin and R.N. Wright, Metall. Trans.A, vol. 22, (1991), 277.
23. J.C.Murray and R.M. German, Advances in Powder Metallurgy, vol.2, (1990), 145.
24. C.E.Lundin, A.S.Yamamoto, Trans.of the Metall.Soc.of AIME, vol.236, (6), (1966), 863.
25. J.L.Jorda, R.Flukiger, and J. Muller, Journal of the Less Common Metals, vol.75, (1980), 227.
26. R.P.Kusy, J.of Applied Physics, vol.48, n° 12, (1977), 530.
27. G.Slama and A.Vignes, J.of Less Common Metals, vol.29, (1972), 189.